

MULTI-ROGUE WAVES AND TRIANGULAR NUMBERS

ADRIAN ANKIEWICZ, NAIL AKHMEDIEV

Optical Sciences Group, Research School of Physics and Engineering,
The Australian National University, Canberra ACT 2600, Australia

Received February 7, 2017

Abstract. Multi-rogue wave solutions of integrable equations have a very specific number of elementary components within their structures. These numbers are given by the “triangular numbers” for the n^{th} -order solution. This contrasts with the case of multi-soliton solutions, where the number of solitons is n . This fact reveals a significant difference between the higher-order rogue waves and the higher-order solitons. Each n^{th} step of generation of multi-rogue wave solutions adds n elementary rogue waves to the solution, in contrast to n -soliton solutions, where each step adds only one soliton to the existing $n - 1$ solitons in the composition. We provide the mathematical analysis for the number of ‘elementary particles’ in the composite rogue wave structures.

Key words: rogue waves; solitons; quanta; triangle numbers.

1. INTRODUCTION

Soliton theory is one of the most important developments in nonlinear dynamics of the twentieth century. It came along with the discovery that a large class of partial differential evolution equations are integrable and that their solutions can be written in analytic form [1–3]. The first equation having that property was found to be the Korteweg-de Vries equation (KdV) [1]. The second equation in this edifice is the nonlinear Schrödinger equation (NLSE) [2]. Many other partial differential evolution equations have been found to be integrable and solvable by the inverse scattering technique and its equivalents [4]. It was commonly believed that the theory of these equations was closed, and most important problems are solved. However, the recent development of solutions describing rogue waves has caused another wave of growing interest in the properties of the NLSE and other similar equations.

Clearly, the set of rogue wave solutions is dramatically different from the set of well-known soliton solutions. Solitons are waves that exist “forever”, at least in their mathematical description. In contrast, rogue waves “appear” and “disappear” [5], and thus are unique formations, both from physical and mathematical points of view. Solitons are present in the initial conditions [1, 2], and the number of them does not change on evolution, no matter how many collisions they experience. Rogue waves, on the other hand, are localized both in time and space. Thus, they do not collide

in the same way as solitons. Their positions are fixed in the spatio-temporal domain and any interaction only occurs due to their decaying tails, unless the positions are very close to each other. We refer the readers to two relevant comprehensive review articles [6, 7].

Another surprising aspect of the set of rogue wave solutions is the patterns of their spatio-temporal positions. The patterns are highly regular, starting right from triangular structures [8, 9] that consist of three Peregrine solutions (PS) [10]. Calculations show [11] that the PSs can be considered as the ‘elementary quanta’ of higher-order structures in the same way that one soliton is an elementary constituent of a multi-soliton solution [2]. An unexpected result here is that the two-Peregrine solution does not exist. The second stage of multi-rogue wave construction leads to three-‘quanta’ solutions; from well-known soliton theory, we may have expected ones with two quanta instead. Moreover, the third step of the mathematical technique produces patterns of six quanta, while in soliton theory, each step adds just one soliton to the total solution. As a result, the number of ‘elementary’ rogue waves (or PSs) in the solution is one of the following numbers: 1, 3, 6, 10, 15 ... etc. This sequence has been found in our previous works [8, 11]. There are no solutions that consist, for example, of 2, 4, 5, 7, ... quanta.

Of course, this fact cannot be revealed simply by observing the complicated profile of the higher-order solutions. The wave interference can make the shape of individual PSs unrecognisable. By analogy, we cannot say how many solitons are in the multi-soliton solution by just looking at the points of soliton collision. Thus, a thorough mathematical analysis is needed.

This unusual property of rogue wave solutions has not been explained so far. In this work, we provide at least a mathematical answer to the following question: why is the number of inherent quanta in a rogue wave pattern given by a triangular number? Although a mathematical answer cannot give physical reasoning for the fact, it provides at least an explanation for the solutions that we have found so far. As we are dealing only with completely integrable systems, the solutions may not entirely describe the reality anyway.

Before entering the details, we should note that rogue waves have been observed experimentally both in optical fibres and water waves [12–15]. Namely, Chabchoub *et al.* [12–14], have experimentally demonstrated the existence of rogue waves of various orders in water. The Peregrine solution in deep water has been observed for the first time in [12], while higher-order rogue waves have been observed in [13, 14, 16]. The first observation of rogue wave triplets is reported in [13]; it is a second-order solution that has the triangular pattern of three separated elementary rogue waves shown in Fig. 1(b) below. Furthermore, rogue waves up to fifth-order are found in water-tank experiments detailed in [14]. For a rogue wave of order n , the expected amplitude is $2n + 1$ [17]. The fact that the amplitudes found were 3,

5, 7, 9 and 11 is a convincing evidence for the physical reality of these higher-order rogue waves.

In optics, the Peregrine solution was first observed by Kibler *et al.* [15]. We stress that we are dealing with the solutions of the fundamental NLSE with no higher-order terms such as third-order dispersion or the Raman effect. The presence of such effects may modify the shapes of the rogue waves but does not influence their very existence. This has been proven experimentally by Hammani *et al.* [18]. The Peregrine solution and even higher-order rogue waves in water are also robust against perturbations [19, 20].

Specifically, in this paper, we consider the NLSE in the following form [21]:

$$i\psi_x + \frac{1}{2}\psi_{tt} + |\psi|^2\psi = 0, \quad (1)$$

where x is the propagation variable and t is time in the moving frame, with the function $|\psi(x, t)|$ being the envelope of the waves. This choice of variables is standard in fibre optics and is now becoming common in nonlinear water wave theory [20, 22].

In the past five years, various ways of deriving higher-order rogue waves (RWs) have been presented [17, 23, 24]. The rogue wave solution of the order n of Eq. (1), in general form, can be written as:

$$\psi_n(x, t) = \left[4 \frac{G_n(x, t) + iK_n(x, t)}{D_n(x, t)} + (-1)^n \right] e^{ix}, \quad (2)$$

where $D_n(x, t)$ is a polynomial of order $n(n+1)$, while $G_n(x, t)$ and $K_n(x, t)$ are polynomials of order $n(n+1) - 2$ and $n(n+1) - 1$, respectively. These values have been found in [17] and presented in the Table 1 of that work. For the 'basic' higher-order rogue waves with all ingredients centred at one point (say, the origin), we can extract a factor x from $K_n(x, t)$, thus leaving a polynomial of order $n(n+1) - 2$.

In the simplest case of the Peregrine solution, where $n = 1$, we have [10, 21]

$$G_1(x, t) = 1, \quad K_1(x, t) = 2x, \quad D_1(x, t) = 1 + 4x^2 + 4t^2. \quad (3)$$

This solution is shown in Fig. 1(a).

A convenient representation of RW solutions appears when the background is extracted from the intensity. Namely, the Peregrine solution can be then written as

$$|\psi_1(x, t)|^2 - 1 = 8 \frac{(1 - 4t^2 + 4x^2)}{(4t^2 + 4x^2 + 1)^2}. \quad (4)$$

We can refer to it as an elementary RW solution (ERW). Equivalently, we can view it as a rogue wave quantum. As we will see from the following, this representation allows us to find the number of ERWs (or quanta) in higher-order RW patterns.

Another interesting fact about this representation is that, for any order n , it can

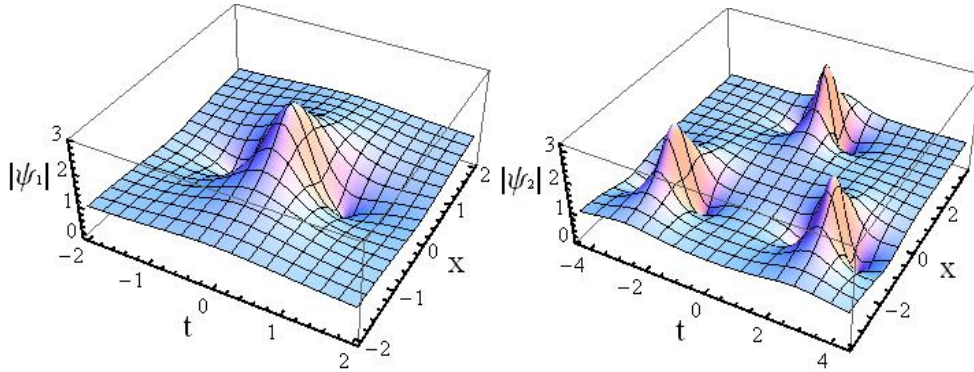


Fig. 1 – (left panel) Single rogue wave described by the Peregrine solution. (right panel) Rogue wave triplet with parameters $\gamma = 200$ and $\beta = 0$ [8, 13].

be expressed in terms of just the denominator of the whole solution [25]:

$$|\psi_n(x, t)|^2 - 1 = [\log(D_n(x, t))]_{tt}. \quad (5)$$

This expression shows that the denominator D_n contains all the information about the intensity patterns of RW solutions.

2. THE NUMBER OF PEREGRINE SOLUTIONS IN HIGHER-ORDER ROGUE WAVE PATTERNS

A general rogue wave pattern is defined by the order of the solution, n , and depends on some free parameters. The free parameters specify mutual separations and relative positions of the individual components on the (x, t) -plane. Generally, a solution of n^{th} order contains $Q_n = n(n+1)/2$ individual components that, when well-separated, can be identified as Peregrine breathers. This is obvious for triangular rogue cascades presented in [26], but not for other patterns. The detailed classification of rogue wave patterns has been given earlier in [11].

It can be inferred that, independent of separation, the n^{th} order pattern always contains $n(n+1)/2$ elementary particles. In other words, solutions of orders $n = 1, 2, 3, 4, 5, \dots$ consist of 1, 3, 6, 10, 15, \dots ERWs respectively. The latter are known as "triangular numbers" illustrated in Fig. 2. These are the total number of points within a triangle with n points along the side of the triangle.

Our aim here is to give an algebraic explanation of the fact that the number of components is defined by the corresponding triangular number. The proof is based on the fact that the denominator of the n^{th} -order rogue wave has order $n(n+1)$, in both x and t and this is the highest order polynomial in the solution. The order of the numerator polynomial must be lower than this. Otherwise, the solution cannot decay

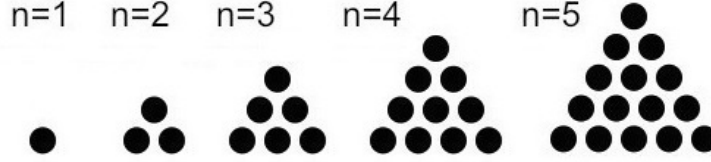


Fig. 2 – The first five triangular numbers. They are represented by the number of solid dots within each triangle.

to the background level at infinity.

Each denominator has no real zeroes, so it cannot be written as a product of $n(n+1)$ linear factors, and its reciprocal has no poles. Thus, each rogue wave has no singularities. So the denominator can only be written as a product of quadratic factors, and there will be $n(n+1)/2$ of them.

The field profile $\psi_n(x, t)$ is dominated by the minima of these quadratic factors. We show here that, no matter how many constant parameters are included into the solution, we can always approximately factor this denominator into a product of $n(n+1)/2$ quadratic polynomials, where each has the form $F_j = 1 + 4(x - x_j)^2 + 4(t - t_j)^2$. As this is the denominator of the Peregrine solution (3), we naturally obtain $n(n+1)/2$ internal PS components that actually can be arranged in various ways in the total pattern [11]. The minima plainly occur at $x = x_j, t = t_j$ for $j = 0, 1, \dots, n-1$. We can use this to determine the dimensions of the full object appearing in the solution in terms of the parameters in the solution.

3. SECOND-ORDER SOLUTIONS (ROGUE WAVE TRIPLETS)

Let us start with the simplest example. The second-order solution with free parameters has been given earlier in [8, 9]. Here we are interested only in the denominator:

$$D_2(x, t) = \beta^2 + \gamma^2 + 64t^6 + 48t^4(4x^2 + 1) - 16\beta t^3 \\ + 12t^2(16x^4 - 24x^2 + 4\gamma x + 9) + 12t\beta(1 + 4x^2) \\ + 64x^6 + 432x^4 - 16\gamma x^3 + 396x^2 - 36\gamma x + 9.$$

Suppose the three components are well separated, i.e. at least one of the parameters β or γ is large. It was shown [8] that the components of the resulting rogue wave triplet are then located at the vertices of an equilateral triangle. Equivalently, we can view them as being located on a circle of large radius, $r = \frac{1}{2\epsilon}$ with 120 degrees angular separation between the components. Thus ϵ is a convenient small parameter. Let us take $\beta = 0$ and $x_1 = \frac{1}{2\epsilon}, x_2 = x_3 = -\frac{1}{4\epsilon}$. Additionally, we set $t_1 = 0, t_2 = -t_3 = \frac{\sqrt{3}}{4\epsilon}$. An example of this solution taken from [8] is shown in Fig. 1(b).

First, we start with special orientations of the triplet on the (x, t) -plane. Let us consider the polynomial $Y = \epsilon^6 [F_1 F_2 F_3 - D_2(x, t)]$, where F_1 , F_2 , and F_3 are three denominators of Peregrine solutions, with their minima located at different places in the (x, t) -plane. Expanding the polynomial Y and taking the γ -value to be large, we can eliminate lower order terms by setting $\gamma = 1/\epsilon^3 + \frac{3}{2\epsilon}$. Then the expression for Y can be written as $Y = 36x\epsilon^3 + \dots$, so the approximation is sufficiently accurate. The replaced denominator solves the NLSE to order ϵ^2 . This means that $\epsilon \approx \gamma^{-1/3} + \frac{1}{2}\gamma$. So the radius of the triplet in Fig. 1(b) is $r = \frac{1}{2}\gamma^{1/3}(1 - \frac{1}{2}\gamma^{-2/3})$. This is an improvement over the estimate given previously in [8].

Now, we rotate the triplet by 90 degrees around the origin. Namely, we consider the case where $\gamma = 0$ with $t_1 = \frac{1}{2\epsilon}$, $t_2 = -t_3 = -\frac{1}{4\epsilon}$, $x_1 = 0$, $x_2 = -x_3 = \frac{\sqrt{3}}{4\epsilon}$. The radius r is the same as before, viz. $\frac{1}{2\epsilon}$. Expanding $Y = \epsilon^6 [F_1 F_2 F_3 - D_2(x, t)]$ and taking β large, we can eliminate lower order terms by setting $\beta = 1/\epsilon^3 + \frac{3}{2\epsilon}$. Then $Y = -12t\epsilon^3 + \dots$, so the approximation is quite accurate. This polynomial also solves the NLSE to order ϵ^2 . This means that $\epsilon \approx \beta^{-1/3} + \frac{1}{2}\beta$. So the radius is $\frac{1}{2}\beta^{1/3}(1 - \frac{1}{2}\beta^{-2/3})$.

For an arbitrary orientation, we can convert $D_2(x, t)$ to radial co-ordinates by setting $t = r \cos(\theta)$ and $x = r \sin(\theta)$. Retaining only the large terms, we find:

$$D_2 \approx 64r^6 + \beta^2 + \gamma^2 - 16r^3[\gamma \cos(3\theta) + \beta \sin(3\theta)].$$

Setting $\frac{\partial}{\partial \theta} D_2$ to zero shows that $\theta = -\frac{1}{3} \arctan(\frac{\beta}{\gamma}) + \frac{2\pi}{3}j$, with $j = 0, 1, 2$. Then setting $\frac{\partial}{\partial r} D_2$ to zero shows that $r = \frac{1}{2}(\beta^2 + \gamma^2)^{1/6}$. This handles any angle of rotation of the triplet in the (x, t) -plane. Similar calculations can be made for the solution of any order, n .

4. CIRCULAR THIRD-ORDER ROGUE WAVE SOLUTION

Now, as a more elaborate example, let us consider the third-order circular rogue wave solution [27]; an example is shown in Fig. 3. This is a particular case of general third-order solution. Forms of the denominator polynomial, $D_3(x, t)$, have been presented earlier in [8, 17, 25, 28] and [29].

The circular pattern is described with a single parameter, b . We can write the denominator with the notations used in [17]:

$$D_3(x, t) = \sum_{j=0}^{12} d_j(T) X^j, \quad (6)$$

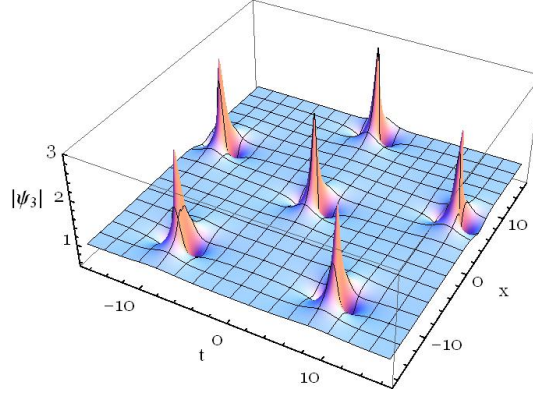


Fig. 3 – Amplitude of third-order RW solution giving circular pattern, found using Eqs. (5) and (6).
Here $b = 2 \times 10^7$.

where $X = 2x$ and $T = 2t$, while the coefficients d_{2j} are:

$$\begin{aligned}
 d_0(T) &= b^2 (T^2 + 1) + T^{12} + 6T^{10} + 135T^8 + 2340T^6 + 3375T^4 + 12150T^2 + 2025, \\
 d_1(T) &= -10b(T^6 - 9T^4 - 45T^2 + 45) \\
 d_2(T) &= b^2 + 6(T^{10} - 15T^8 + 90T^6 + 2250T^4 - 6075T^2 + 15525), \\
 d_3(T) &= 10b(T^4 + 18T^2 + 9), \\
 d_4(T) &= 15(T^8 - 12T^6 - 90T^4 + 5220T^2 + 9585), \\
 d_5(T) &= 6b(3T^2 - 17), \\
 d_6(T) &= 20(T^6 + 3T^4 + 675T^2 + 765), \\
 d_7(T) &= -2b, \\
 d_8(T) &= 15(T^4 + 18T^2 + 249), \\
 d_{10}(T) &= 6(T^2 + 21), \\
 d_{12}(T) &= 1,
 \end{aligned}$$

with $d_9(T) = d_{11}(T) = 0$. If b is large, then the central part is described by

$$D_3(x, t) = b^2(1 + T^2 + X^2) = b^2(1 + 4t^2 + 4x^2),$$

as expected for a single ERW at the origin. When $b = 0$, D_3 reduces to the form given in Appendix E of [17] (with numerators and denominators multiplied by 16200). Since D_3 has order 12, at large b , we can approximately factor it into a product of six polynomials, $\prod_{j=0}^5 F_j$, representing six separated ERWs. For a circular pattern [27], one of them is centred at the origin and the remaining five form a pentagon around it, as shown in Fig. 3.

Thus, we have the expected total of six inherent ERWs with one in the middle and other five located equidistantly on a circle with radius r .

5. APPROXIMATIONS FOR HIGHER-ORDER CIRCULAR ROGUE WAVE PATTERNS

For simplicity, let us again consider only the circular solutions [27], and find the radii r of these circles. Then we only need to minimize D_n for large values of (x, t) . In other words, we need to find the value of r that minimizes D_n . This step involves only a few higher order terms in the polynomial. As before, we set $X = 2x$. For $n = 3$, the terms of highest order in X are

$$D_3 = X^{12} - 2bX^7 + b^2X^2 + \dots$$

Setting $b = (2u_3r)^5$ with $x = r, t = 0$ for example, shows that $(u_3^5 - 1)^2r^{12} = 0$, so $u_3 = 1$ and the radius is $r \approx \frac{1}{2}b^{1/5}$. Figure 3 uses $b = 2 \times 10^7$, and it can be seen that the predicted radius of 14.4 is quite accurate.

For $n = 4$, the terms of highest order in X are

$$D_4 = X^{20} - 2bX^{13} + b^2X^6 + \dots$$

Setting $b = (2u_4r)^7$ with $x = r, t = 0$ for example, shows that $(u_4^7 - 1)^2r^{20} = 0$, so $u_4 = 1$ and the radius is $r \approx \frac{1}{2}b^{1/7}$. Near the centre, i.e for x, t small, for b large, we see that

$$\begin{aligned} D_3/b^2 &\approx 9 + 27T^2 + 3T^4 + T^6 + 99X^2 + 27X^4 + X^6 - 18T^2X^2 \\ &+ 3T^4X^2 + 3T^2X^4, \end{aligned}$$

where $T = 2t$, i.e. it is the form of a second order basic rogue wave, given in [30] (see also [5, 17]). This is an algebraic verification of the inherent quanta referred to earlier. Here, the central 2^{nd} order rogue wave contains three quanta, while each of the seven in the surrounding ring contains one, making the expected total of ten.

For $n = 5$, the terms of highest order are $D_5 = X^{30} + 2bX^{21} + b^2X^{12} + \dots$. Setting $b = (2u_5r)^9$ with $x = -r, t = 0$ for example, shows that $(u_5^9 - 1)^2r^{30} = 0$, so $u_5 = 1$ and the radius is $r \approx \frac{1}{2}b^{1/9}$.

For $n = 6$, the terms of highest order are $D_6 = X^{42} - 2bX^{31} + b^2X^{20} + \dots$. Setting $b = (2u_6r)^{11}$ with $x = r, t = 0$ for example, shows that $(u_6^{11} - 1)^2r^{42} = 0$, so $u_6 = 1$ and the radius is $r \approx \frac{1}{2}b^{1/11}$. For general n , the radius is $r \approx \frac{1}{2}b^{1/(2n-1)}$.

6. INTEGRAL DEFINING THE NUMBER OF ERWS IN THE PATTERN

The above radius estimates are approximate. However, from the above study, it clearly appears that the number of ERWs does not depend on the free parameters at all. Their relative locations can change, and the position of each individual ERW may move, but the total number of them remains fixed and is given by a triangular number. Moreover, all ERWs can be built into a structure which does not allow us to see each part separately. However, even such a complicated structure consists of a fixed number of ERWs given by a triangular number [31].

Can this fact be expressed explicitly and with mathematical accuracy in the form of an integral? We claim that indeed it can.

We propose that the number of components can be calculated as the integral of the squared deviation from the background level across the space-time plane, i.e.

$$\frac{1}{8\pi} \int_{-\infty}^{\infty} \int_{-\infty}^{\infty} (|\psi_n(x,t)|^2 - 1)^2 dt dx = \frac{1}{2}n(n+1) = Q_n. \quad (7)$$

In other words, the number of components Q_n (either explicitly visible or not) is

$$Q_n = \frac{1}{8\pi} \int_{-\infty}^{\infty} \int_{-\infty}^{\infty} ([\log(D_n(x,t))]_{tt})^2 dt dx.$$

As follows from (7), for the multi-rogue wave solution $\psi_n(x,t)$ of order n , the integral will be equal to a triangular number of order n , *viz.* Q_n . This integral does not depend on the free parameters included in the solution $\psi_n(x,t)$. Numerical evidence shows that the above integral is always equal to the number of ERWs in the solution, no matter what kind of pattern it has.

Again, let us start with the simplest case. If we consider a single Peregrine solution, $\psi_1(x,t)$, we obtain analytically from Eq. (4):

$$\int_{-\infty}^{\infty} [|\psi_1(x,t)|^2 - 1]^2 dt = \frac{8\pi}{(1+4x^2)^{3/2}}.$$

and then:

$$\int_{-\infty}^{\infty} (1+4x^2)^{-3/2} dx = 1,$$

so that the number of components $Q_1 = 1$, as conjectured.

For higher-order solutions, if the rogue wave components are 'well-separated' into a certain structure with $\frac{1}{2}n(n+1)$ peaks (i.e. the solution parameters are large), then Q_n will plainly be the sum of the integrals over each individual peak. As each integral equals unity, so $Q_n = \frac{1}{2}n(n+1)$.

When separation is only partial (i.e. the solution parameters are small), then we can expand the integrand to first-order in a small parameter. Consider the 2^{nd} order rogue wave of Sec. 3, and let the integrand in Eq. (7) be $g(x,t,\beta,\gamma)$. For $\gamma = 0$ and β small, this can be expanded as $g(x,t,0,0) + \beta \frac{\partial g}{\partial \beta}$. The surface integral of the first part is three; the second function is odd in t for each x and hence the integral of it is zero. Similarly, for γ small and $\beta = 0$, we have $g(x,t,\beta=0,\gamma) = g(x,t,0,0) + \gamma \frac{\partial g}{\partial \gamma} + \dots$. The latter term is odd in x for any t , so the integral of it is zero. So Q_2 remains equal to three as separation commences. The same effect occurs for the 3^{rd} order rogue wave of Sec. 4. The value of Q_3 remains equal to six as b starts to increase.

A further clue as to the reason for this particular form of the integral comes from the fact that, when parameters are set to zero, the intensity at the origin is found

from

$$|\psi_n(0,0)|^2 - 1 = c_n = 4n(n+1).$$

This follows from the fact that the maximal possible amplitude of the solution is at the origin and is given by $\psi_n(0,0) = (2n+1)$ [17, 32]. Suppose that the integrand is approximated by a smooth function with this maximum at the centre and decaying at infinity. To be definite, let us take a gaussian with amplitude c_n^2 , i.e.

$$S_n = c_n^2 \exp(-c_n r^2),$$

where $r^2 = x^2 + t^2$. Then

$$\frac{1}{8\pi} (2\pi) \int_0^\infty S_n r dr = \frac{c_n}{8} = \frac{1}{2} n(n+1) = Q_n. \quad (8)$$

This is the same result as in Eq. (7). Thus, we find that the value of Q_n is closely related to the central maximum of the integrand.

This is a fundamental result: *the number of ERWs in a multi-rogue wave solution of the NLSE is given by a triangular number*. No other number of ERWs can be present in a general multi-rogue wave solution.

Moreover, the number of ERWs can be found from the integral for all higher-order solutions, including those where the rogue waves of order n are only partially 'separated' into elementary components. In these cases, the number of ERWs is not visually obvious. This integral can be used to determine the number of ERWs in any unknown rogue wave pattern.

Clearly, this approach can be applied only to solutions localized both in time and in space. Otherwise the integral may become infinite. Clearly, no such integral can be proposed for soliton solutions. This mere fact shows once again the crucial differences that exist between the classes of soliton solutions and rogue wave solutions.

7. DIFFERENCE IN CONSTRUCTION OF MULTI-SOLITONS AND MULTI-ROGUE WAVES

To demonstrate the crucial difference between solitons and RWs more clearly, let us recall that, at any step n of construction of multi-soliton solutions, we add one more soliton to the existing $n-1$ solitons added up in the previous steps. This happens when we use the Darboux transformation scheme or any other dressing technique known from the literature. Thus, at each step, we move from an $(n-1)$ -soliton solution to a higher-order n -soliton solution. Then the number of solitons in the construction is equal to the order of the solution.

On the other hand, building a multi-rogue wave solution is different. At the n^{th} step of construction, we add not one but n ERWs to the already-existing pattern. In

particular, the first step provides us with a solution containing just one ERW. In the second step, we add two ERWs to the first-order solution, thus obtaining a solution with three ERWs. In the third step, we add three more ERWs, thus obtaining a pattern with six ERWs. This is equivalent to building a triangle, layer-by-layer, starting from one as the vertex, thus increasing the total number of ERWs in this particular way. So, it is not too surprising that the total number of ERWs in the pattern is defined by the triangular number of the order n . This can be visualised when looking at the sequence of triangles of increasing order, as shown in Fig. 2.

8. CONCLUSION

To conclude, firstly, we have given a simple algebraic method to understand the number of components existing in higher-order rogue waves of the NLSE. This helps in understanding the patterns that can occur. Secondly, we have proposed an integral that can be used to determine this number for a given higher-order rogue wave pattern. Thirdly, we provided simple rules to visualise the process of building up higher-order rogue wave solutions and explained why the number of elementary quanta is given by a “triangular number”. Based on these rules, we have demonstrated the crucial difference between the multi-soliton and multi-rogue wave solutions.

Other integrable equations have multi-rogue wave solutions that are similar to those of the NLSE. To name a few, we can mention Hirota equation [33], Kundu-DNLS equation [34], derivative NLSE [35, 36], coupled NLSE [37, 38], Kundu-Eckhaus equation [39], Sasa-Satsuma equation [40], Fokas-Lenells equation [41], resonant three-wave interaction problem [42, 43] and other higher-order extensions of the NLSE [44, 45]. Recently, other significant papers on these topics have been published [46–51]. The principles developed in this present work could potentially find a wide range of applicability in physical systems.

Acknowledgements. The authors acknowledge the support of the Australian Research Council (Discovery Project numbers DP140100265 and DP150102057) and support from the Volkswagen Stiftung.

REFERENCES

1. C. S. Gardner, J. M. Greene, M. D. Kruskal, and R. M. Miura, *Method for Solving the Korteweg-de Vries Equation*, Phys. Rev. Lett. **19**, 1095–1097 (1967).
2. V. E. Zakharov and A. B. Shabat, *Exact theory of two-dimensional self-focusing and one-dimensional self-modulation of waves in nonlinear media*, Journal of Experimental and Theoretical Physics, **34**, 62–69 (1972).
3. M. J. Ablowitz, D. J. Kaup, A. C. Newell, and H. Segur, *The Inverse Scattering Transform - Fourier Analysis for Nonlinear Problems*, Stud. Appl. Math. **53**, 249–315 (1974).

4. M. Ablowitz and P. Clarkson, *Solitons, Nonlinear Evolution Equations and Inverse Scattering*, Cambridge University Press, Cambridge, 1991.
5. N. Akhmediev, A. Ankiewicz, and M. Taki, *Waves that appear from nowhere and disappear without a trace*, Phys. Lett. A, **373**, 675–678 (2009).
6. M. Onorato, S. Residori, U. Bortolozzo, A. Montina, and F. T. Arecchi, *Rogue waves and their generating mechanisms in different physical contexts*, Phys. Rep. **528**, 47–89 (2013).
7. N. Akhmediev *et al.*, *Roadmap on optical rogue waves and extreme events*, J. Opt. **18**, 063001 (2016).
8. A. Ankiewicz, D. J. Kedziora, and N. Akhmediev, *Rogue wave triplets*, Phys. Lett. A **375**, 2782–2785 (2011).
9. P. Dubard, P. Gaillard, C. Klein, and V. B. Matveev, *On multi-rogue wave solutions of the NLS equation and positon solutions of the KdV equation*, Eur. Phys. J. Special Topics **185**, 247–258 (2010).
10. D. H. Peregrine, *Water waves, nonlinear Schrödinger equations and their solutions*, J. Australian Math. Soc., Series B **25**, 16–43 (1983).
11. D. J. Kedziora, A. Ankiewicz, and N. Akhmediev, *Classifying the hierarchy of nonlinear Schrödinger equation rogue wave solutions* Phys. Rev. E **88**, 013207 (2013).
12. A. Chabchoub, N. P. Hoffmann, and N. Akhmediev, *Rogue wave observation in a water wave tank*, Phys. Rev. Lett. **106**, 204502 (2011).
13. A. Chabchoub and N. Akhmediev, *Observation of rogue wave triplets in water waves*, Phys. Lett. A **377**, 2590–2593 (2013).
14. A. Chabchoub, N. Hoffmann, M. Onorato, A. Slunyaev, A. Sergeeva, E. Pelinovsky, and N. Akhmediev, *Observation of a hierarchy of up to fifth-order rogue waves in a water tank*, Phys. Rev. E **86**, 056601 (2012).
15. B. Kibler, J. Fatome, C. Finot, G. Millot, F. Dias, G. Genty, N. Akhmediev, and J. M. Dudley, *The Peregrine soliton in nonlinear fibre optics*, Nature Physics **6**, 790–795 (2010).
16. A. Chabchoub, N. P. Hoffmann, M. Onorato, and N. Akhmediev, *Super Rogue Waves: Observation of a Higher-Order Breather in Water Waves*, Phys. Rev. X **2**, 011015 (2012).
17. N. Akhmediev, A. Ankiewicz, and J. M. Soto-Crespo, *Rogue waves and rational solutions of the nonlinear Schrödinger equation*, Phys. Rev. E **80**, 026601 (2009).
18. K. Hammani, B. Kibler, Ch. Finot, Ph. Morin, J. Fatome, J. M. Dudley, and G. Millot, *Peregrine soliton generation and breakup in standard telecommunications fiber*, Opt. Lett. **36**, 112–114 (2011).
19. A. Chabchoub, N. Hoffmann, H. Branger, C. Kharif, and N. Akhmediev, *Experiments on wind-perturbed rogue wave hydrodynamics using the Peregrine breather model*, Physics of Fluids **25**, 101704 (2013).
20. A. Slunyaev, E. Pelinovsky, A. Sergeeva, A. Chabchoub, N. Hoffmann, M. Onorato, and N. Akhmediev, *Super-rogue waves in simulations based on weakly nonlinear and fully nonlinear hydrodynamic equations*, Phys. Rev. E **88**, 012909 (2013).
21. N. Akhmediev and A. Ankiewicz, *Solitons, nonlinear pulses and beams*, Chapman and Hall, London, 1997.
22. A. Osborne, *Nonlinear Ocean Waves and the Inverse Scattering Transform*, Academic Press, Elsevier, Amsterdam, 2010.
23. Y. Ohta and J. Yang, *General high-order rogue waves and their dynamics in the nonlinear Schrödinger equation*, Proc. R. Soc. A **468**, 1716–1740 (2012).
24. J. S. He, H. R. Zhang, L. H. Wang, K. Porsezian, and A. S. Fokas, *Generating mechanism for higher-order rogue waves*, Phys. Rev. E **87**, 052914 (2013).

25. Liming Ling and Li-Chen Zhao, *Simple determinant representation for rogue waves of the nonlinear Schrödinger equation*, Phys. Rev. E **88**, 043201 (2013).
26. D. J. Kedziora, A. Ankiewicz, and N. Akhmediev, *Triangular rogue wave cascades*, Phys. Rev. E **86**, 056602 (2012).
27. D. J. Kedziora, A. Ankiewicz, and N. Akhmediev, *Circular rogue wave clusters*, Phys. Rev. E **84**, 056611 (2011).
28. P. Gaillard, *Deformations of third-order Peregrine breather solutions of the nonlinear Schrödinger equation with four parameters*, Phys. Rev. E **88**, 042903 (2013).
29. P. Gaillard, *Degenerate determinant representation of solutions of the nonlinear Schrödinger equation, higher order Peregrine breathers and multi-rogue waves*, J. Math. Phys. **54**, 013504 (2013).
30. N. N. Akhmediev, V. M. Eleonskii, and N. E. Kulagin, *Generation of periodic trains of picosecond pulses in an optical fiber: Exact solutions*, Sov. Phys. JETP **62**, 894–899 (1985).
31. A. Ankiewicz and N. Akhmediev, *Multi-rogue waves and triangle numbers*, Australian and New Zealand Conference on Optics and Photonics (Adelaide, South Australia, 2015), Engineers Australia/Australian Optical Society, ISBN: 9781922107664.
32. A. Ankiewicz, P. A. Clarkson, and N. Akhmediev, *Rogue waves, rational solutions, the patterns of their zeros and integral relations*, J. Phys. A: Math. Theor. **43**, 122002 (2010).
33. A. Ankiewicz, J. M. Soto-Crespo, and N. Akhmediev, *Rogue waves and rational solutions of the Hirota equation*, Phys. Rev. E **81**, 046602 (2010).
34. Shibao Shan, Chuanzhong Li, and Jingsong He, *On rogue wave in the Kundu-DNLS equation*, Commun. Nonlinear Sci. Numer. Simulat. **18**, 3337–3349 (2013).
35. Boling Guo, Liming Ling, and Q. P. Liu, *High-Order Solutions and Generalized Darboux Transformations of Derivative Nonlinear Schrödinger Equations*, Stud. Appl. Math. **130**, 317–344 (2012).
36. Yongshuai Zhang, Lijuan Guo, Shuwei Xu, Zhiwei Wu, and Jingsong He, *The hierarchy of higher order solutions of the derivative nonlinear Schrödinger equation*, Commun. Nonlinear Sci. Numer. Simulat. **19**, 1706–1722 (2014).
37. F. Baronio, A. Degasperis, M. Conforti, and S. Wabnitz, *Solutions of the vector nonlinear Schrödinger equations: Evidence for deterministic rogue waves*, Phys. Rev. Lett. **109**, 044102 (2012).
38. Bao-Guo Zhai, Wei-Guo Zhang, Xiao-Li Wang, and Hai-Qiang Zhang, *Multi-rogue waves and rational solutions of the coupled nonlinear Schrödinger equations*, Nonlinear Analysis: Real World Applications **14**, 14–27 (2013).
39. Xin Wang, Bo Yang, Yong Chen, and Yunqing Yang, *Higher-order rogue wave solutions of the Kundu-Eckhaus equation*, Phys. Scr. **89**, 095210 (2014).
40. U. Bandelow and N. Akhmediev, *Persistence of rogue waves in extended nonlinear Schrödinger equations: Integrable Sasa – Satsuma case*, Phys. Lett. A **376**, 1558 (2012).
41. Shuwei Xua, Jingsong He, Yi Chenga, and K. Porseizan, *The n-order rogue waves of Fokas-Lenells equation*, Math. Meth. Appl. Sci. **38**, 1106–1126 (2015).
42. F. Baronio, M. Conforti, A. Degasperis, and S. Lombardo, *Rogue Waves Emerging from the Resonant Interaction of Three Waves*, Phys. Rev. Lett. **111**, 114101 (2013).
43. S. Chen, J. M. Soto-Crespo, and Ph. Grelu, *Watch-hand-like optical rogue waves in three-wave interactions*, Opt. Express **23**, 349–359 (2015).
44. Bo Yang, Wei-Guo Zhang, Hai-Qiang Zhang, and Sheng-Bing Pei, *Generalized Darboux transformation and rogue wave solutions for the higher-order dispersive nonlinear Schrödinger equation*, Phys. Scr. **88**, 065004 (2013).
45. A. Ankiewicz, Yan Wang, S. Wabnitz, and N. Akhmediev, *Extended nonlinear Schrödinger equa-*

- tion with higher-order odd and even terms and its rogue wave solutions*, Phys. Rev. E **89**, 012907 (2014).
46. S. Chen and D. Mihalache, *Vector rogue waves in the Manakov system: diversity and compossibility*, J. Phys. A: Math. Theor. **48**, 215202 (2015).
 47. S. Chen, J. M. Soto-Crespo, F. Baronio, Ph. Grelu, and D. Mihalache, *Rogue-wave bullets in a composite $(2 + 1)D$ nonlinear medium*, Opt. Express **24**, 15251–15260 (2016).
 48. S. Chen, P. Grelu, D. Mihalache, and F. Baronio, *Families of rational soliton solutions of the Kadomtsev-Petviashvili I equation*, Rom. Rep. Phys. **68**, 1407–1424 (2016).
 49. S. W. Xu, K. Porsezian, J. S. He, and Y. Cheng, *Multi-optical rogue waves of the Maxwell-Bloch equations*, Rom. Rep. Phys. **68**, 316–340 (2016).
 50. F. Yuan, J. Rao, K. Porsezian, D. Mihalache, and J. S. He, *Various exact rational solutions of the two-dimensional Maccari's system*, Rom. J. Phys. **61**, 378–399 (2016).
 51. Y. Liu, A. S. Fokas, D. Mihalache, and J. S. He, *Parallel line rogue waves of the third-type Davey-Stewartson equation*, Rom. Rep. Phys. **68**, 1425–1446 (2016).